Supporting Information for

Aviation-Related Impacts on Ultrafine Particle Number Concentrations Outside and Inside Residences near an Airport

N. Hudda[1]*, M.C. Simon[1,2], W. Zamore[3] and J.L. Durant[1]

[1] Tufts University, Department of Civil and Environmental Engineering, 200 College Ave, 204 Anderson Hall, Medford, MA 02155, USA.

[2] Boston University, Department of Environmental Health, 715 Albany Street, Boston, MA 02118, USA.

[3]Somerville Transportation Equity Partnership, 13 Highland Ave. #3, Somerville, MA 02143, USA.

*Corresponding Author

Email: neelakshi.hudda@tufts.edu

Address: Department of Civil and Environmental Engineering, 200 College Ave, 204 Anderson Hall, Tufts University, Medford, MA 02155, USA.

Tel: 617.627.5489

Fax: 617.627.3994

Google Scholar Profile: https://scholar.google.com/citations?user=xA1QrtwAAAAJ&hl=en

Number of Pages: 34

Number of Figures: 53

Number of Tables: 6

Information Related to Flight Activity at Logan International Airport

Diurnal Flight Activity Patterns

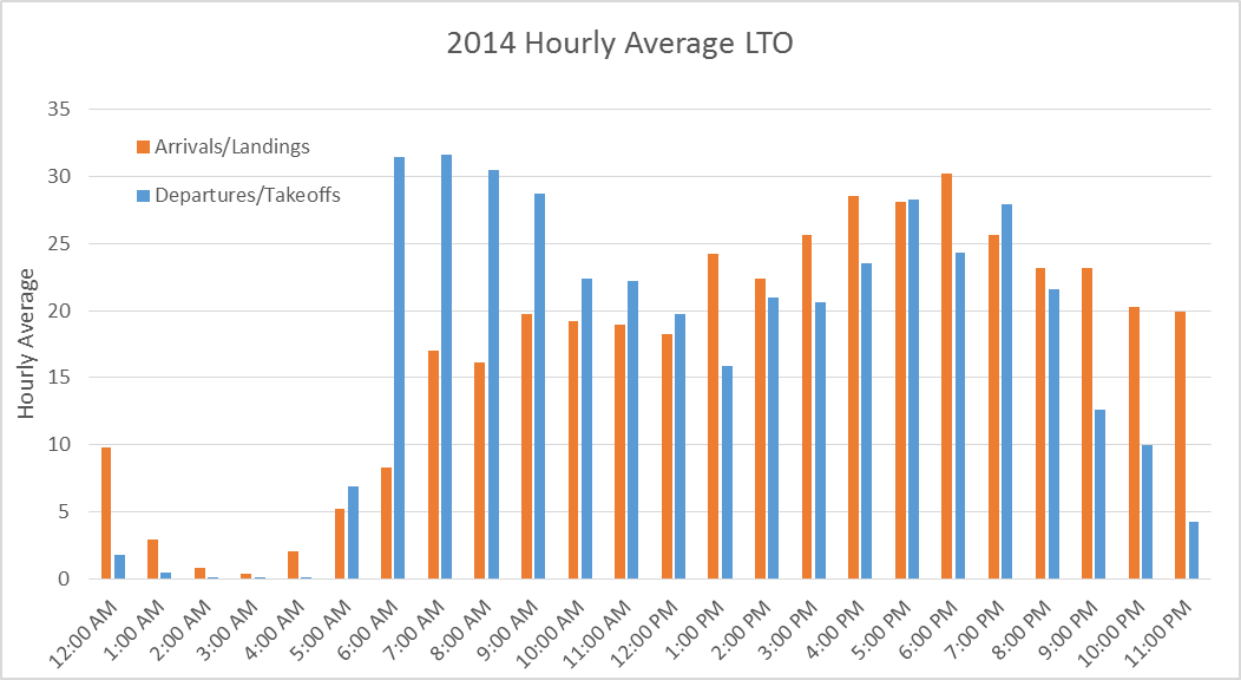

Figure S1: Annual (2014) average of hourly totals for landings and takeoffs through the day.

Monitoring Schedule and Data Summary

Chelsea Study Area

Table S1: Monitoring schedule at Chelsea residential sites and summary of meteorological parameters during monitoring.

ID	Monitoring Period	Total Hours	Temp (°C)	Relative Humidity (%)	LTO (number/h)	WS (km/h)
U1	07/10/2014-08/21/2014	1008	21 ± 4	68 ± 18	36 ± 20	14 ± 6
U2	04/30/2014-06/11/2014	1009	15 ± 5	66 ± 20	36 ± 21	16 ± 7
D1	10/28/2014-12/09/2014	1007	6 ± 6	63 ± 23	34 ± 20	18 ± 8
D2	02/06/2014-03/20/2014	1000	-2 ± 5	54 ± 21	33 ± 20	17 ± 8
C1	08/01/2014-09/11/2014	962	20 ± 7	63 ± 24	33 ± 20	15 ± 6
C2	04/03/2014-05/15/2014	1005	11 ± 5	60 ± 20	37 ± 21	18 ± 9
C3	10/02/2014-11/14/2014	1031	12 ± 5	70 ± 21	35 ± 21	17 ± 9

Table S2: Impact sector definitions and summary of particle number concentration statistics for Chelsea residential sites.

ID	Distance To airport (km)	Impact Sector Definition (WD°)	Impact Sector Frequency, Hours	Median of Impact-sector Hourly Statistics			Median of Other Winds Hourly Medians		
				Outdoor Median	Indoor Median	Indoor Minimum	Outdoor	Indoor	Indoor Minimum
U1	4.9	142 - 176	5.3%, 53	14900	2300	1400	7800	1900	1600
U2	4.0	117 - 164	11.8%, 119	18600	2500	1800	10700	2400	1800
D1	4.3	111 - 155	4.7%, 47	36000	11100	7600	13200	4400	3700
D2	4.4	111 - 154	5%, 50	37100	14600	7500	16200	5100	3500
C1	4.2	145 - 182	5.2%, 50	12800	3500	2800	8100	2500	1900
C2	4.4	130 - 171	5.4%, 54	19700	1900	1300	9700	2200	1700
C3	3.7	124 - 173	10.8%, 111	26600	6400	4700	8900	2800	2200

Table S3: Residence characteristics and distance of residences from major roadways in Chelsea.

ID	Housing Type	Location of Indoor Monitor	Cooking Stove Type	Nearest Major Roadway (m)	Distance to US-1 (m)	Distance to MA-16 (m)
U1	apartment	living room	gas	27	27	80
U2	apartment	living room	electric	190	200	1300
D1	apartment	living room	electric	130	130	1300
D2	apartment	living room	electric	220	210	1300
C1	apartment	bedroom	gas	110	810	570
C2	apartment	bedroom	electric	320	320	680
C3	apartment	living room	electric	330	570	1400

Boston Study Area

Table S4: Monitoring schedule at Boston residential sites and summary of meteorological parameters during monitoring.

ID	Monitoring Period	Total Hours	Temp (°C)	Relative Humidity (%)	LTO (number/h)	WS (km/h)
D1	09/27/2012-11/06/2012	913	12 ± 4	70 ± 18	35 ± 23	15 ± 7
U1	10/24/2012-12/04/2012	935	6 ± 4	69 ± 16	25 ± 17	16 ± 8
U2	05/07/2012-06/20/2012	853	17 ± 4	73 ± 19	38 ± 24	15 ± 7
C1	06/17/2013-07/29/2013	1006	24 ± 5	72 ± 17	44 ± 26	15 ± 6
C2	08/05/2013-09/16/2013	1008	21 ± 5	64 ± 20	43 ± 26	15 ± 6
C3	09/10/2013-10/21/2013	984	16 ± 4	69 ± 16	42 ± 27	14 ± 7
B1	04/18/2013-05/30/2013	1006	13 ± 4	68 ± 21	41 ± 26	17 ± 8
B2	06/07/2013-07/22/2013	1080	23 ± 6	71 ± 18	43 ± 25	16 ± 6
B3	06/21/2012-08/02/2012	986	23 ± 5	63 ± 18	31 ± 21	14 ± 6

Table S5: Impact sector definitions and summary of particle number concentration statistics for Boston residential sites.

ID	Distance To airport (km)	Impact Sector Definition (WD°)	Impact Sector Winds Fraction (%), Hours	Median of Impact-sector Hourly Statistics			Median of Other Winds Hourly Statistics		
				Outdoor Median	Indoor Median	Indoor Minimum	Outdoor	Indoor	Indoor Minimum
D1	6.1	31 - 59	6.9%, 63	27800	8400	4300	10700	5300	4000
U1	5.0	28 - 61	8.4%, 79	25100	22700	17500	14700	7400	6100
U2	5.6	30 - 59	8.2%, 70	19700	10900	6900	9700	6100	3700
C1	6.8	53 - 79	9.6%, 97	9400	3700	2600	8000	2300	1800
C2	7.1	53 - 78	3%, 30	11900	7900	6400	10000	4100	2800
C3	7.8	62 - 86	9.6%, 94	21000	7700	5800	14300	3900	3300
B1	10.0	33 - 53	3.4%, 34	13500	4900	4200	10100	4500	3400
B2	8.8	48 - 67	6%, 65	8200	4900	3200	7200	4500	3000
B3	9.2	60 - 78	4%, 39	12900	15400	11600	8100	6300	5100

Table S6: Residence characteristics and distance of residences from major roadways in Boston.

ID	Housing Type	Location of Indoor Monitor	Cooking Stove Type	Nearest Major Roadway (m)	Distance to I-93 (m)	Distance to I-90 (m)
D1	apartment	living room	electric	200	200	2400
U1	apartment	living room	gas	310	880	1900
U2	apartment	living room	electric	230	230	2200
C1	apartment	bedroom	gas	110	1400	1100
C2	apartment	living room	gas	110	1600	1300
C3	apartment	living room	electric	120	2800	480
B1	apartment	living room	electric	14	1900	4600
B2	apartment	bedroom	gas	54	3100	3000
B3	apartment	living room	gas	26	3800	1800

Illustration of Impact-sector determination

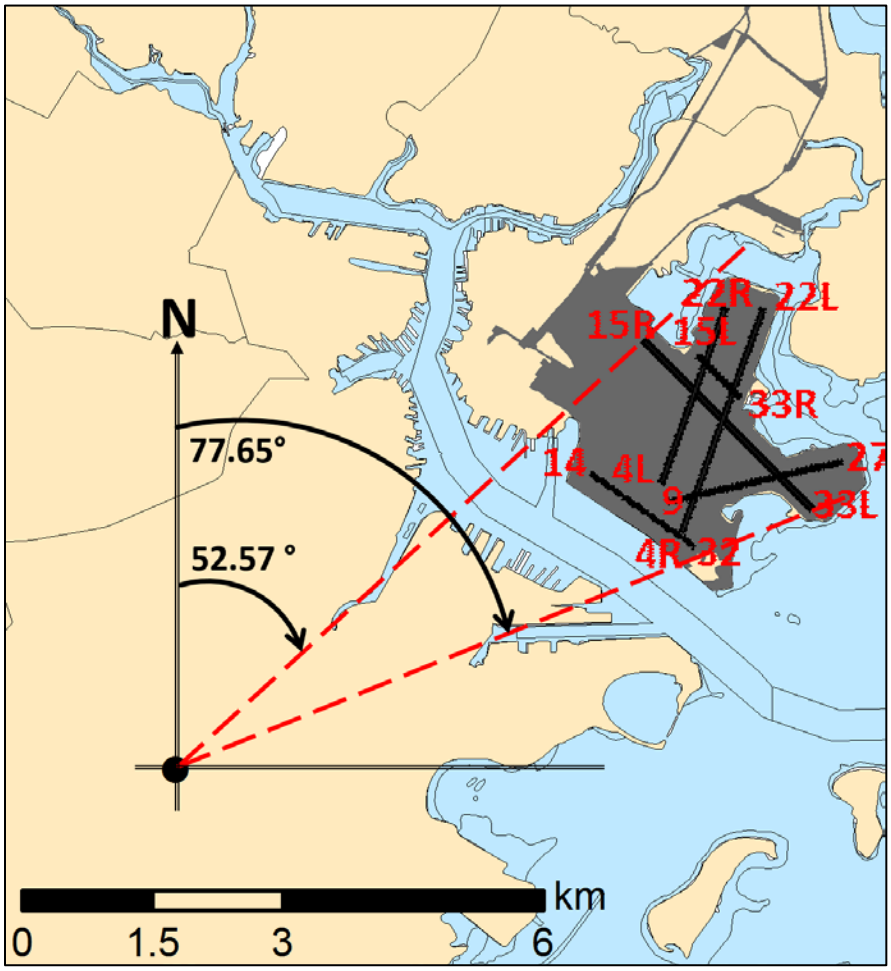

Figure S2: Determination of impact-sector for the Boston central site.

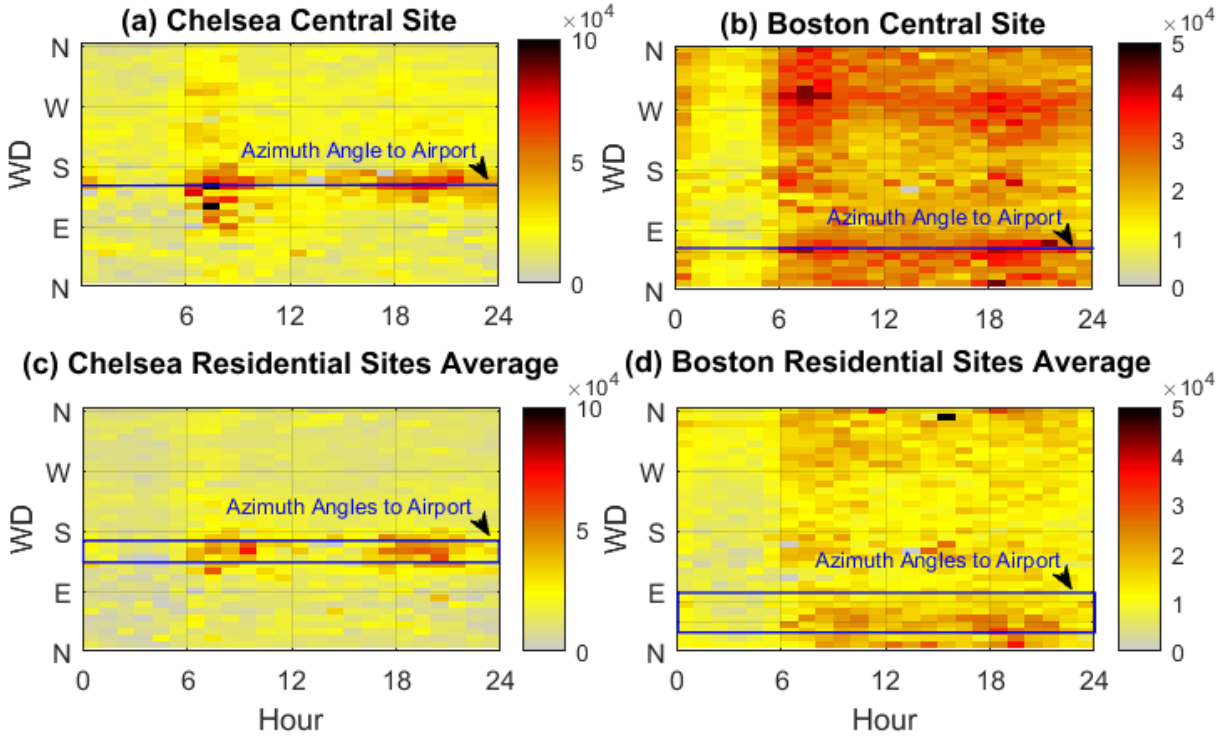

Figure S3: Heat maps of PNC at the central sites (a,b) and all residential sites (c,d) by wind direction and hour of the in Chelsea (a,c) and Boston (b,d).

Bootstrap Correlation Coefficient Estimates between Particle Number Concentration and Wind Speed

Impact-sector winds dataset at residences were relatively small; they ranged from 30-119 h or 3.0%-11.8% of the total data. To ensure that the results were not by chance and to take the resulting uncertainty due to small sample size into account, we compared distributions of correlation coefficient estimates generated using bootstrap resampling method (1×10^4 random samples with replacement) for impact-sector winds to other winds. Subsamples (1×10^4 random samples without replacement) from other-winds dataset but of size comparable to impact-sector-winds have also been compared in the following Figures S4-S10 and S11-S19 for all Chelsea and Boston residences. Only the significant correlation estimates (p-value < 0.05) of the 1×10^4 estimates are plotted in the following figures.

In Chelsea, at six of the seven homes, the distribution of Spearman's correlation coefficient estimates for impact sector winds was in the positive range and different from the distribution of estimates for other winds which was in the negative range with almost no overlap between the distributions. Site D2 was an exception (see Figure S7 with a complete overlap between the distributions. It is possible that since site is downwind of a highway during impact-sector winds, the dominant impact at this site is of the highway emissions and not the airport. Nonetheless, even in the overlapping distributions, correlation estimates were less negative during impact-sector winds compared to other winds. However, at site D1 that is also downwind of the same highway during impact-sector winds and we did not observe a complete overlap between impact-sector and other-wind correlation estimates, though a small fraction of the 1×10^4 estimates was in the same range as the estimates for other winds (see Figure S6).

In the Boston study area, at the two sites upwind of I-93 (U1 and U2), the correlation estimates were very different for impact-sector compared to other winds (see Figure S12 & 13). At site D1, downwind of I-93, there was a complete overlap between the two (see Figure S11). At other 6 homes, the results were mixed. Impact-sector vs other winds estimates were different when comparing bootstrap resampling estimates; there was little to no overlap between the range of the distributions. But when comparing impact-sector resampling estimates with other wind subsampling estimates, i.e., when subsamples that were equally small as impact-sector winds were drawn from the distributions for other winds, the differences were small and there was overlap in the range of the distributions.

Chelsea Study Area

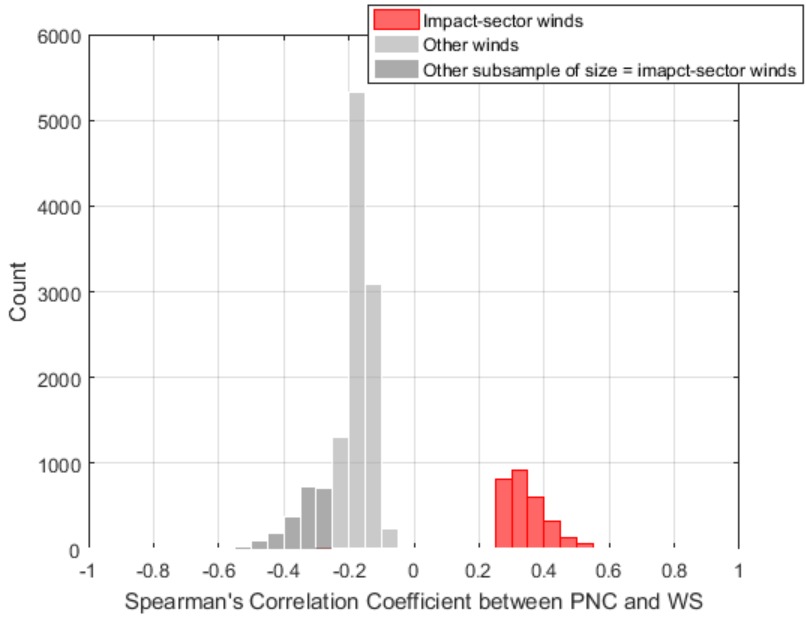

Figure S4: Distribution of bootstrap estimates for Spearman's correlation coefficient between PNC and WS at site U1.

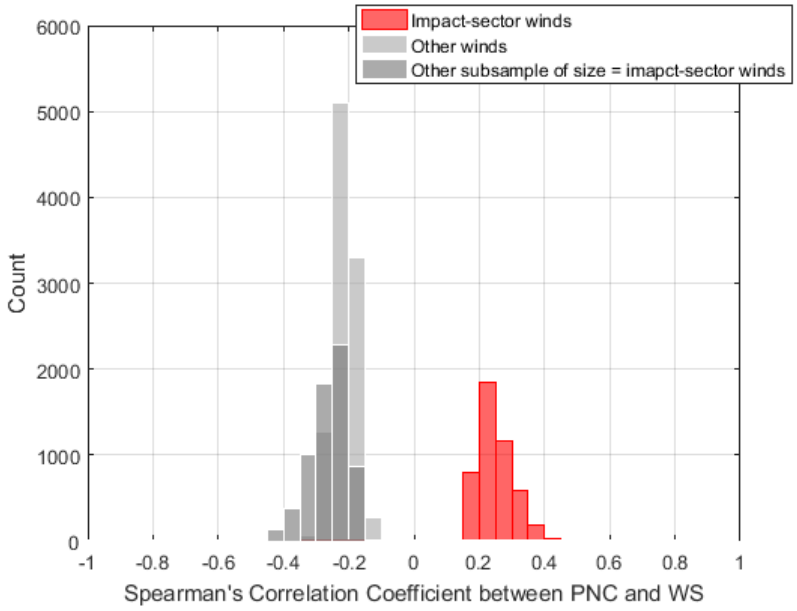

Figure S5: Distribution of bootstrap estimates for Spearman's correlation coefficient between PNC and WS at site U2.

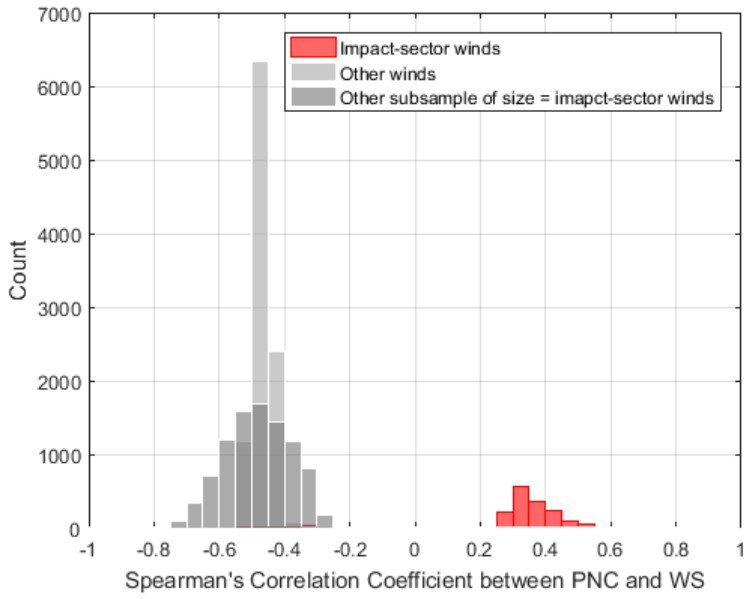

Figure S6: Distribution of bootstrap estimates for Spearman's correlation coefficient between PNC and WS at site D1.

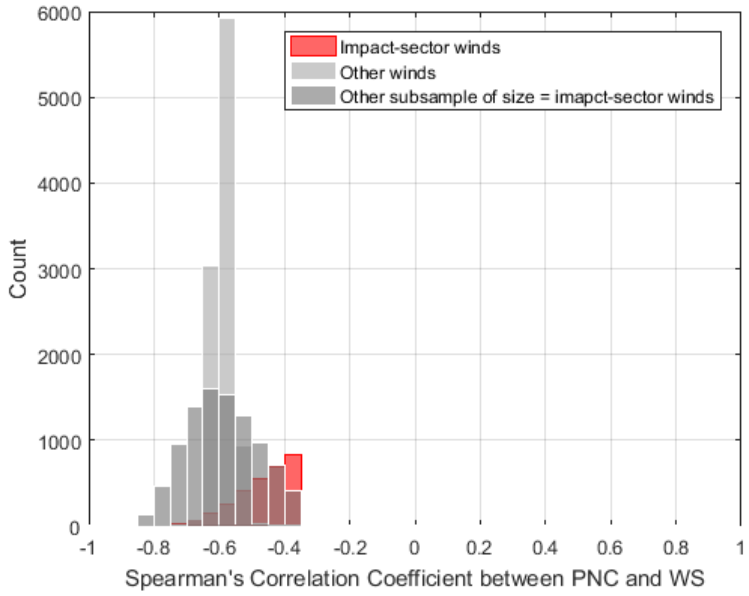

Figure S7: Distribution of bootstrap estimates for Spearman's correlation coefficient between PNC and WS at site D2.

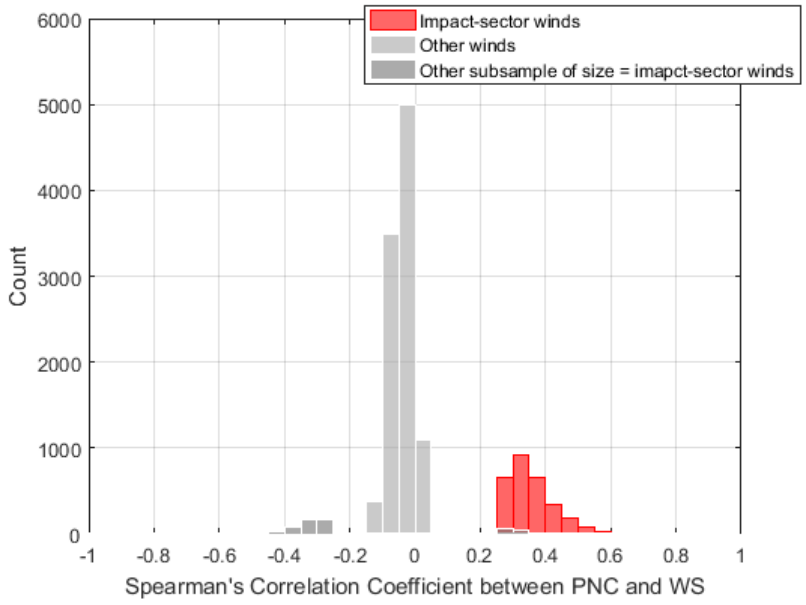

Figure S8: Distribution of bootstrap estimates for Spearman's correlation coefficient between PNC and WS at site C1.

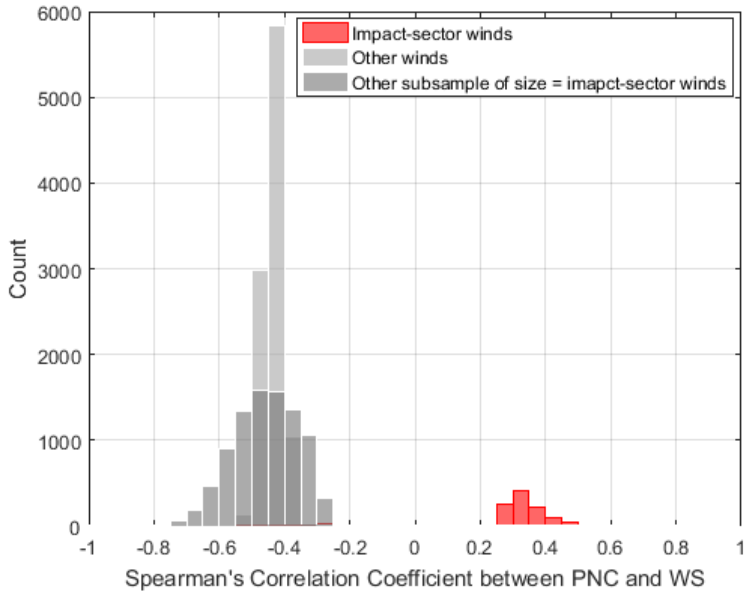

Figure S9: Distribution of bootstrap estimates for Spearman's correlation coefficient between PNC and WS at site C2.

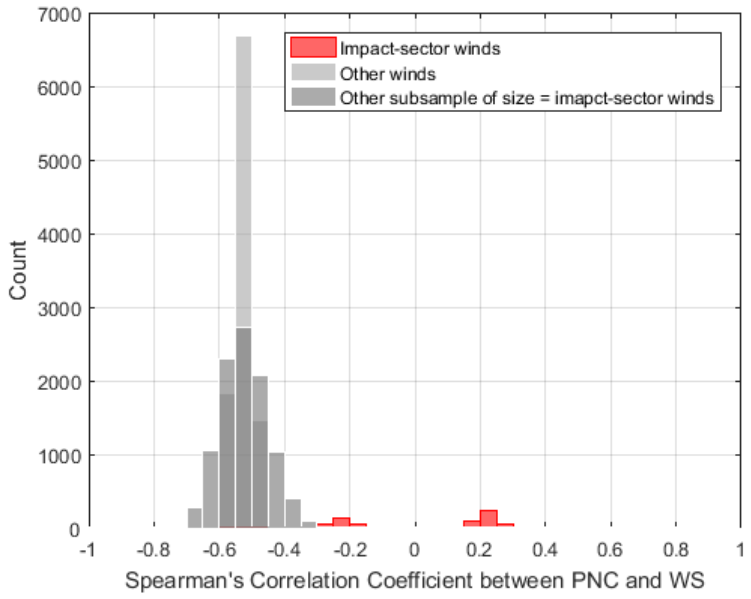

Figure S10: Distribution of bootstrap estimates for Spearman's correlation coefficient between PNC and WS at site C3.

Boston Study Area

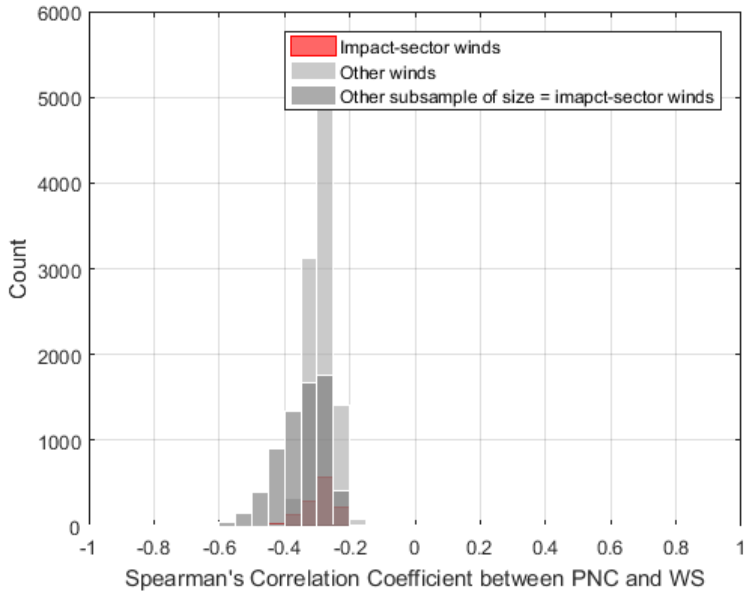

Figure S11: Distribution of bootstrap estimates for Spearman's correlation coefficient between PNC and WS at site D1.

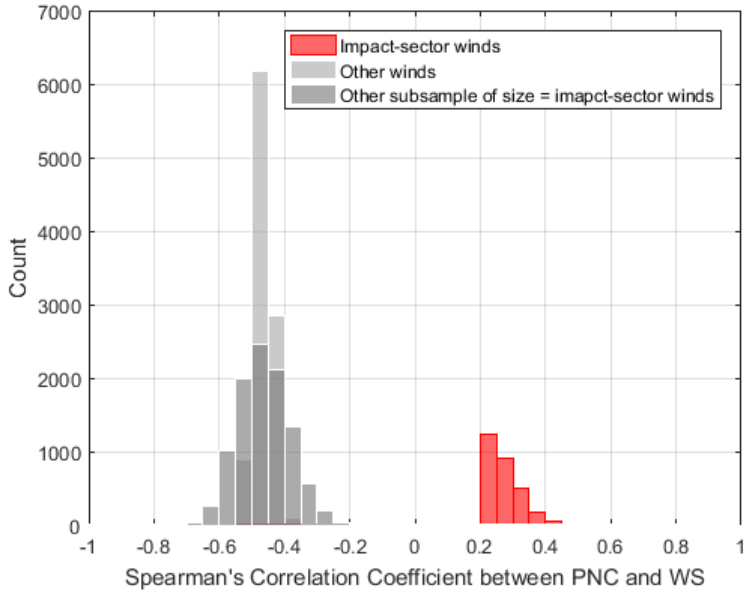

Figure S12: Distribution of bootstrap estimates for Spearman's correlation coefficient between PNC and WS at site U1.

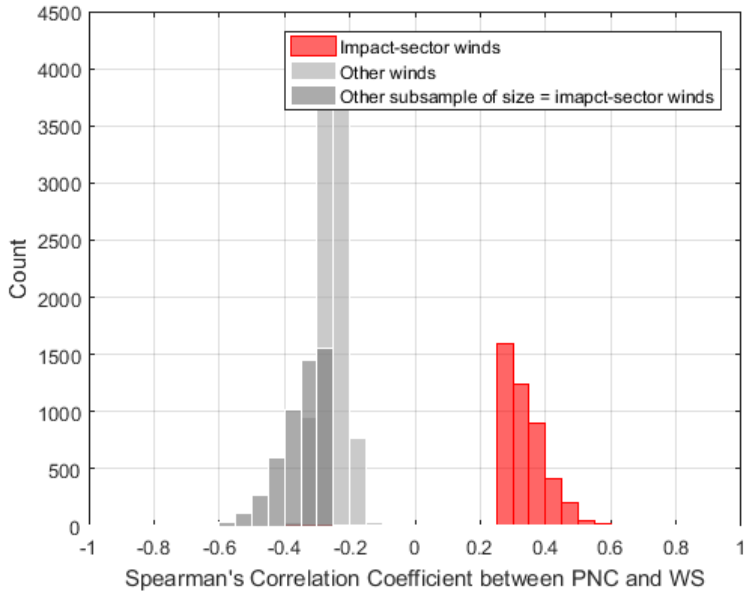

Figure S13: Distribution of bootstrap estimates for Spearman's correlation coefficient between PNC and WS at site U2.

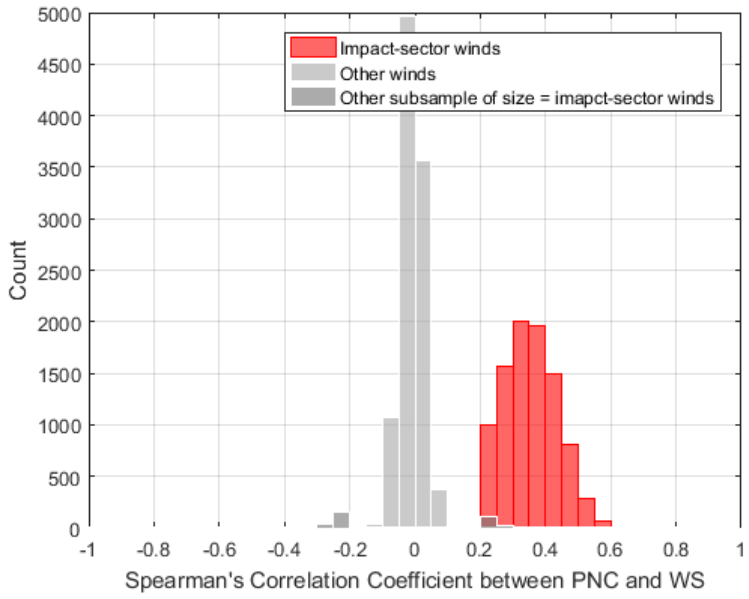

Figure S14: Distribution of bootstrap estimates for Spearman's correlation coefficient between PNC and WS at site C1.

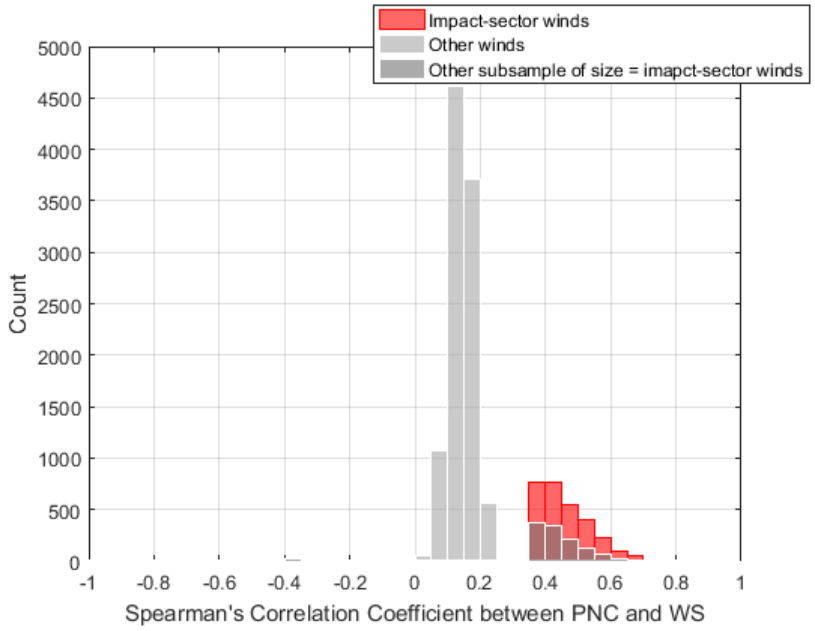

Figure S15: Distribution of bootstrap estimates for Spearman's correlation coefficient between PNC and WS at site C2.

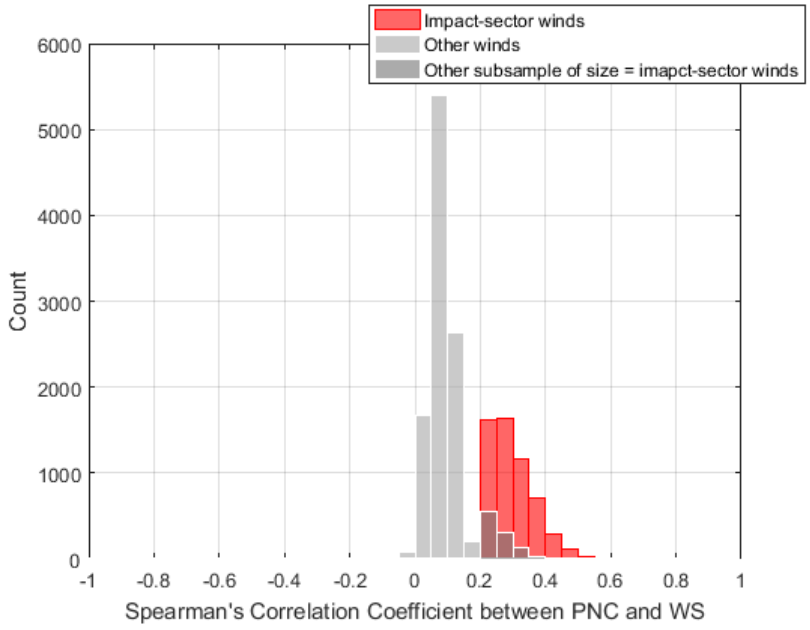

Figure S16: Distribution of bootstrap estimates for Spearman's correlation coefficient between PNC and WS at site C3.

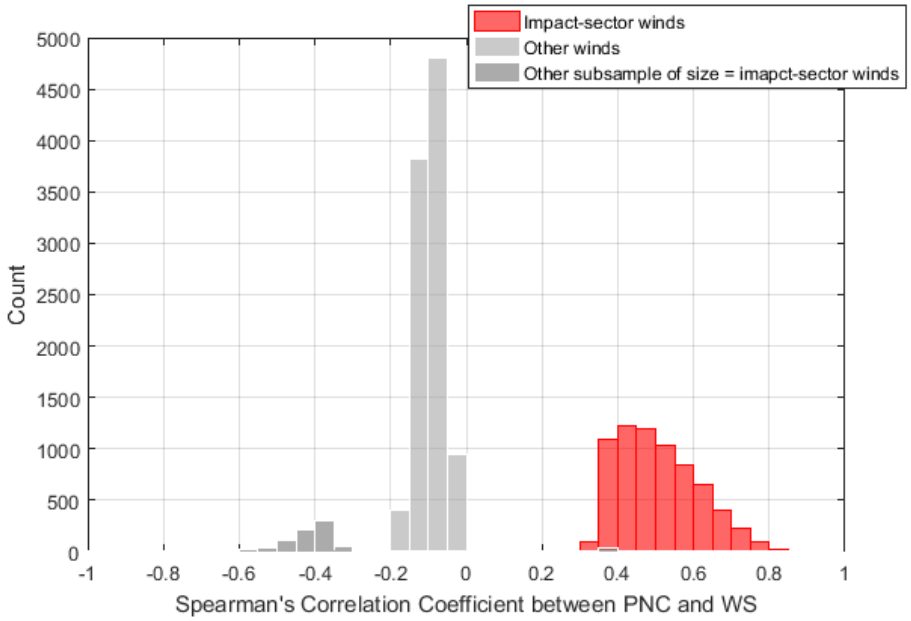

Figure S17: Distribution of bootstrap estimates for Spearman's correlation coefficient between PNC and WS at site B1.

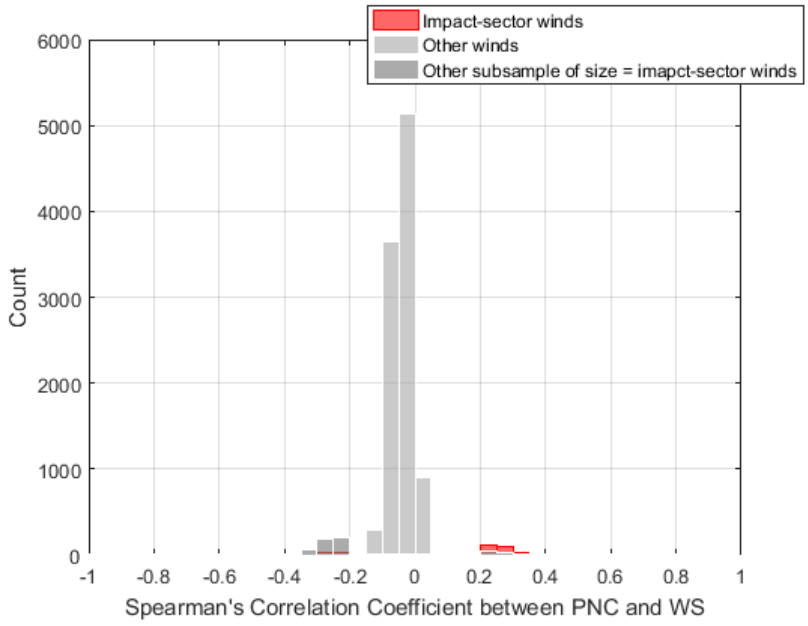

Figure S18: Distribution of bootstrap estimates for Spearman's correlation coefficient between PNC and WS at site B2.

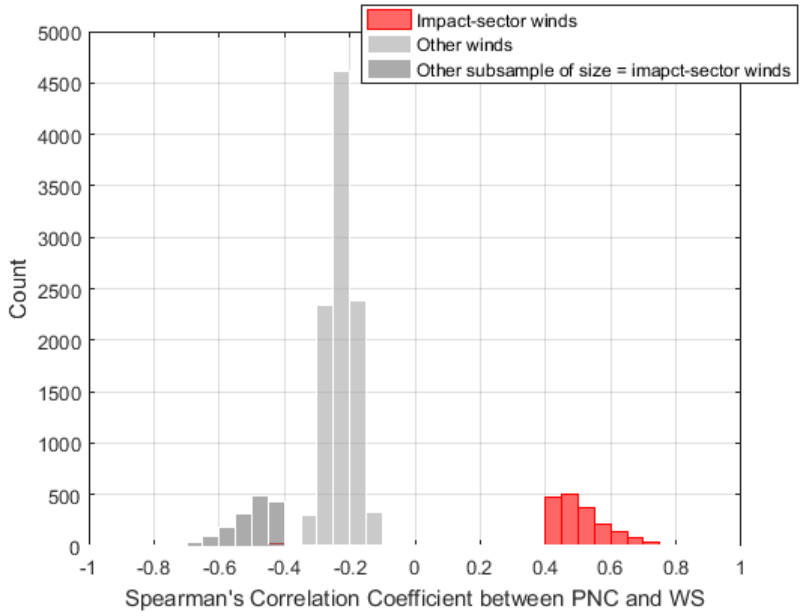

Figure S19: Distribution of bootstrap estimates for Spearman's correlation coefficient between PNC and WS at site B3.

Bootstrap Correlation Coefficient Estimates between Particle Number Concentration and Flight Activity

We have compared distributions of Spearman's correlation coefficient estimates generated using bootstrap resampling methods (1×10^4 random samples with replacement) for impact-sector winds to other winds in the following Figures S20-S26 and S27-S35 for all Chelsea and Boston residences. Only the significant correlation estimates (p-value < 0.05) of the 1×10^4 estimates are plotted in the following figures.

For all but one Chelsea home (D2), the range of Spearman's correlation estimates for impact-sector winds had some overlap with estimates for other winds but the median (even mode) of the distribution was still higher for impact-sector winds than other winds. For site D2, we observed a complete overlap (see Figure S23). Site D2 was also an exception to the trend observed for PNC and wind speed correlations. For the Boston homes, generally, correlation estimates were higher during impact-sector winds but results were mixed for some sites. For sites C2, C3, and B3, the distributions of correlation estimates were not different between impact-sector and other winds.

Chelsea Study Area

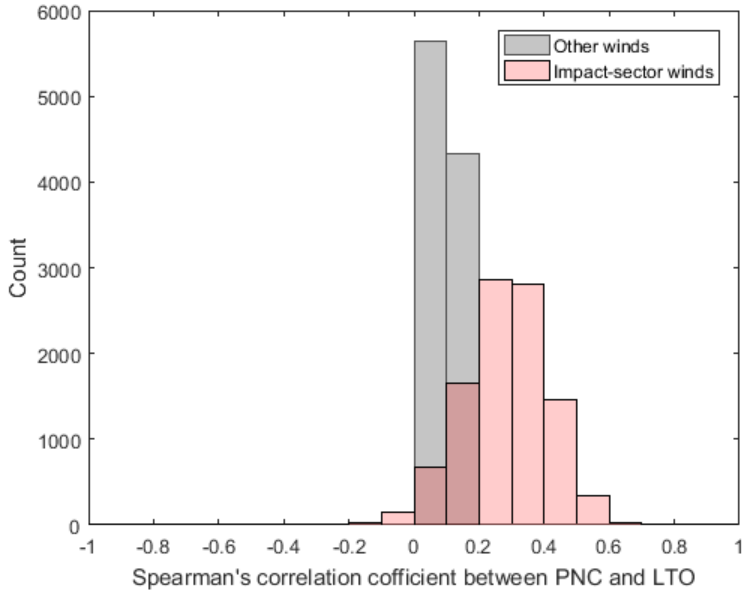

Figure S20: Distribution of bootstrap estimates for Spearman's correlation coefficient between PNC and WS at site U1.

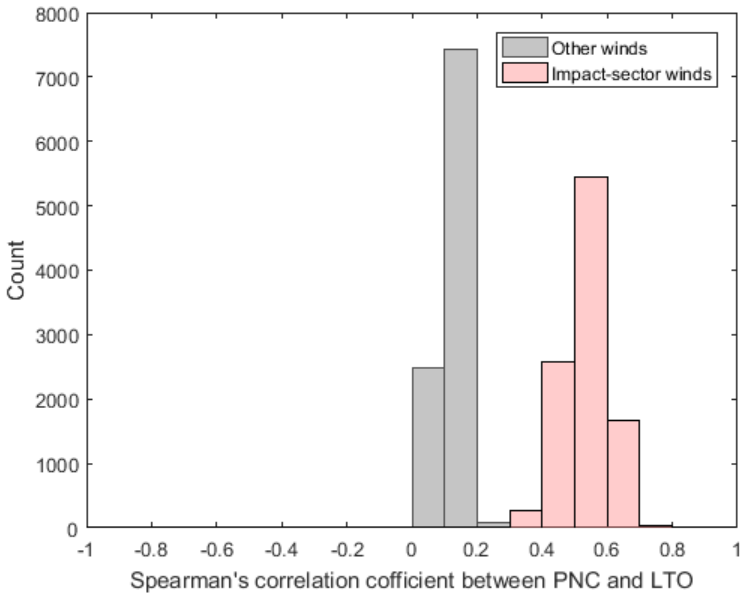

Figure S21: Distribution of bootstrap estimates for Spearman's correlation coefficient between PNC and WS at site U1.

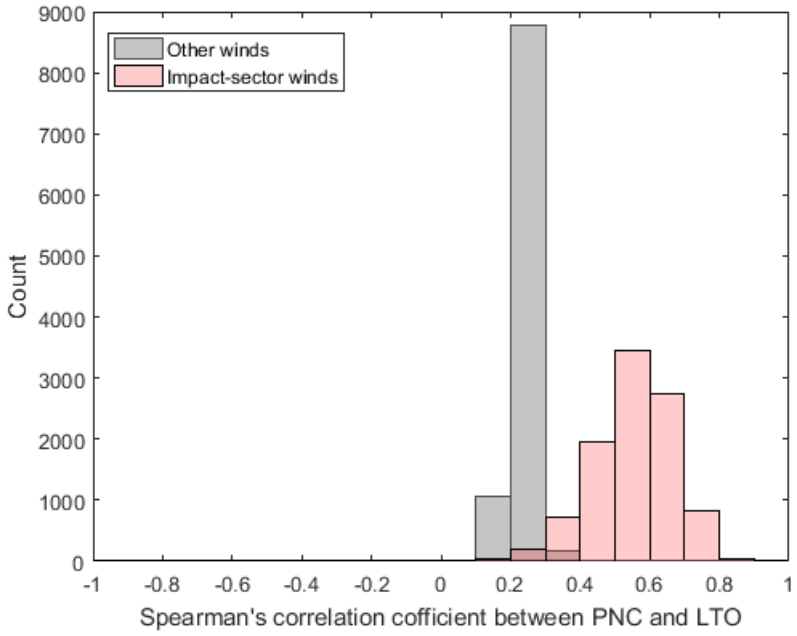

Figure S22: Distribution of bootstrap estimates for Spearman's correlation coefficient between PNC and WS at site D1.

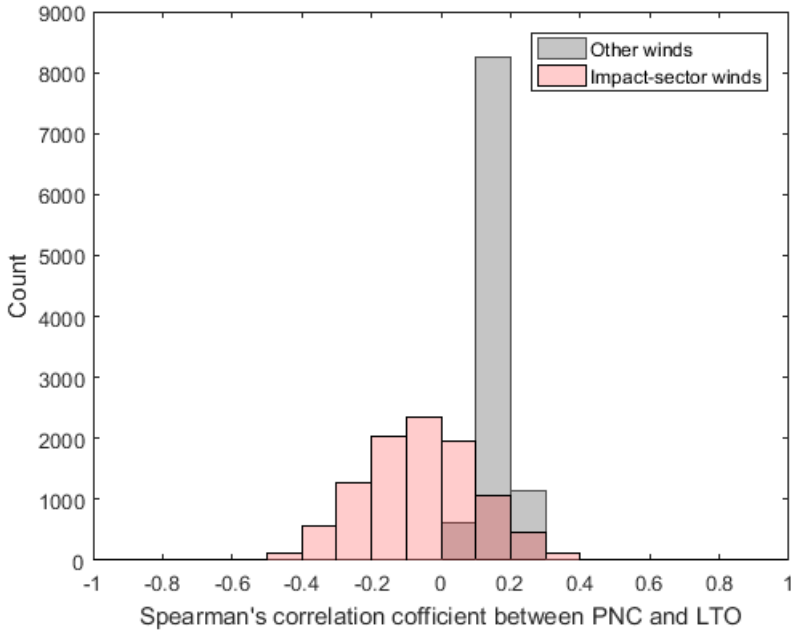

Figure S23: Distribution of bootstrap estimates for Spearman's correlation coefficient between PNC and WS at site D2.

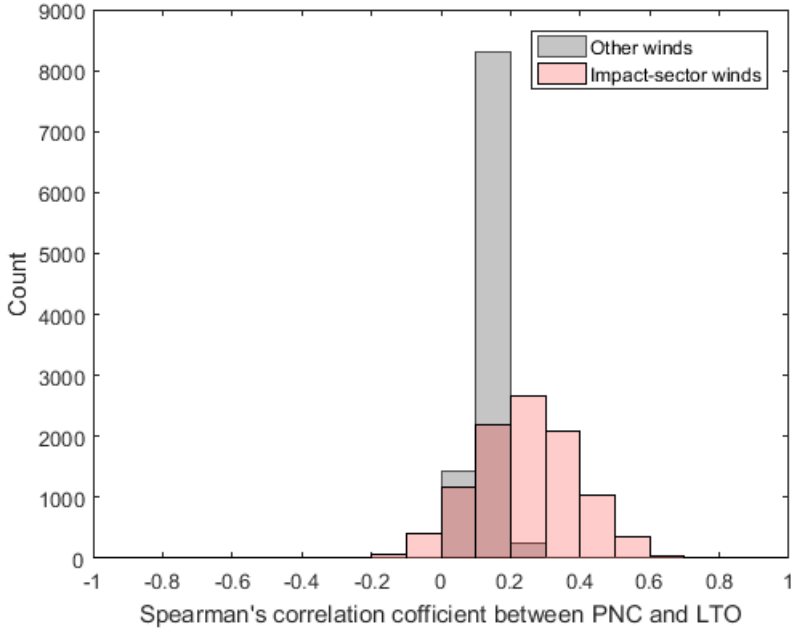

Figure S24: Distribution of bootstrap estimates for Spearman's correlation coefficient between PNC and WS at site C1.

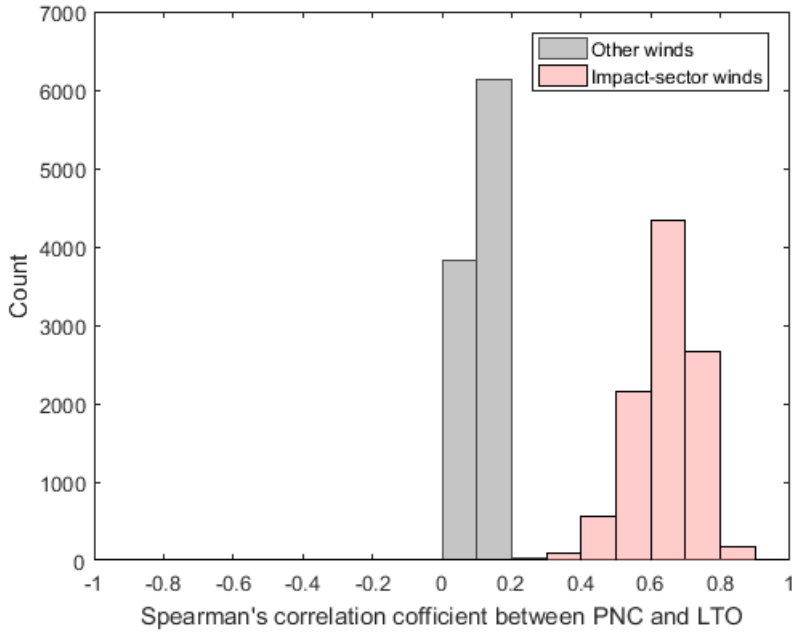

Figure S25: Distribution of bootstrap estimates for Spearman's correlation coefficient between PNC and WS at site C2.

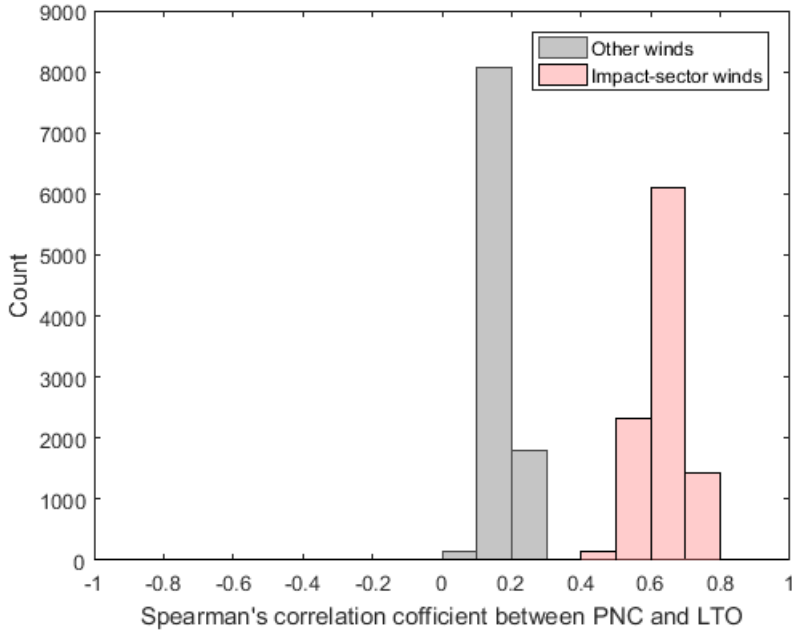

Figure S26: Distribution of bootstrap estimates for Spearman's correlation coefficient between PNC and WS at site C3.

Boston Study Area

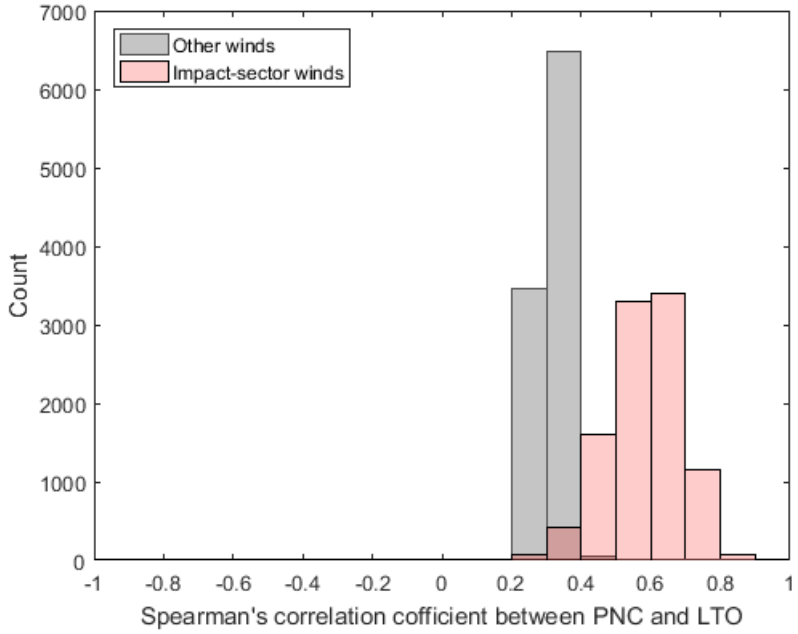

Figure S27: Distribution of bootstrap estimates for Spearman's correlation coefficient between PNC and WS at site D1.

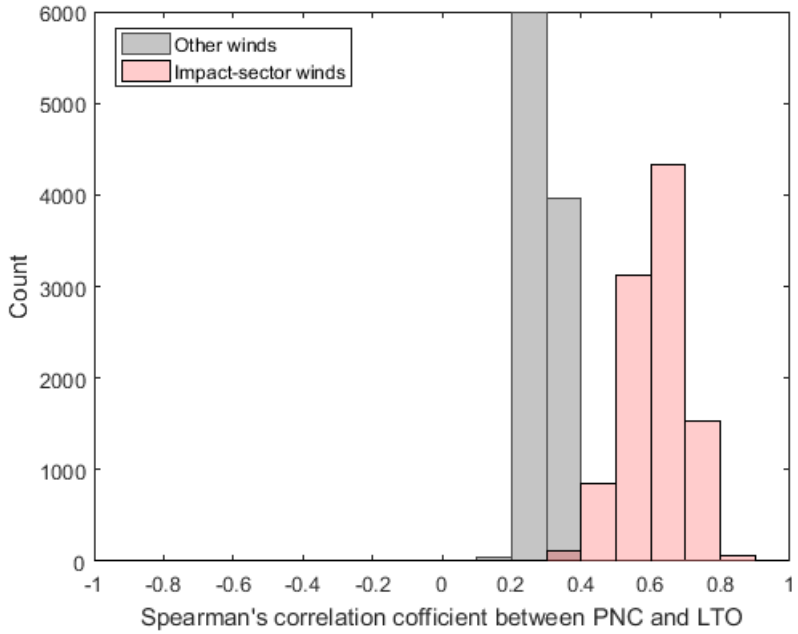

Figure S28: Distribution of bootstrap estimates for Spearman's correlation coefficient between PNC and WS at site U1.

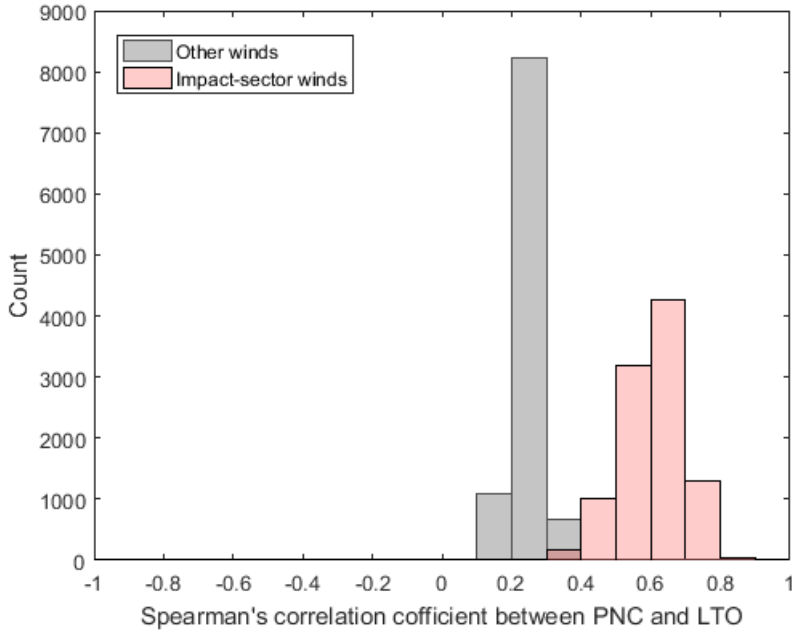

Figure S29: Distribution of bootstrap estimates for Spearman's correlation coefficient between PNC and WS at site U2.

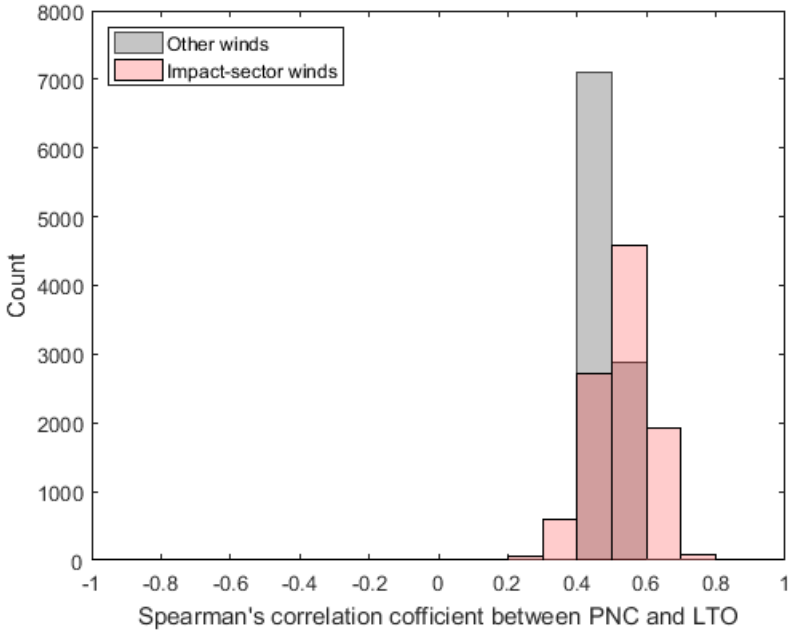

Figure S30: Distribution of bootstrap estimates for Spearman's correlation coefficient between PNC and WS at site C1.

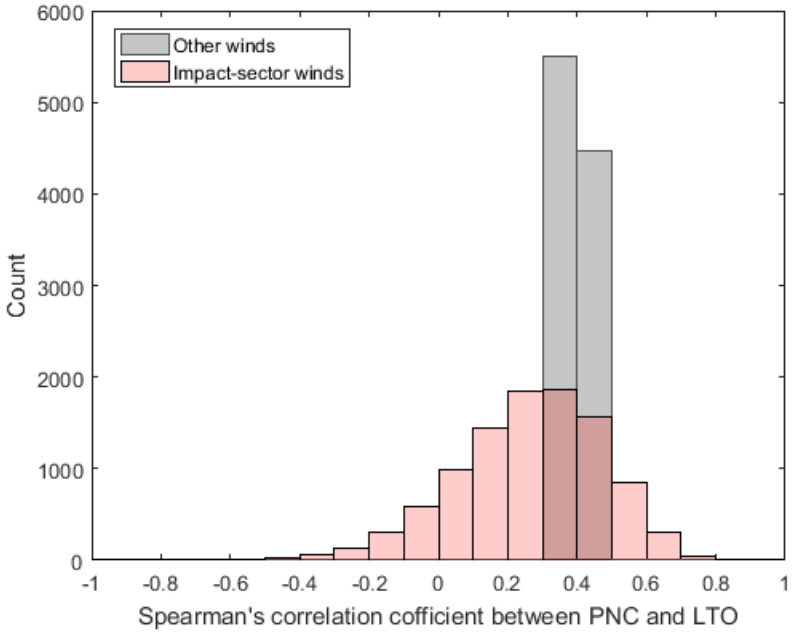

Figure S31: Distribution of bootstrap estimates for Spearman's correlation coefficient between PNC and WS at site C2.

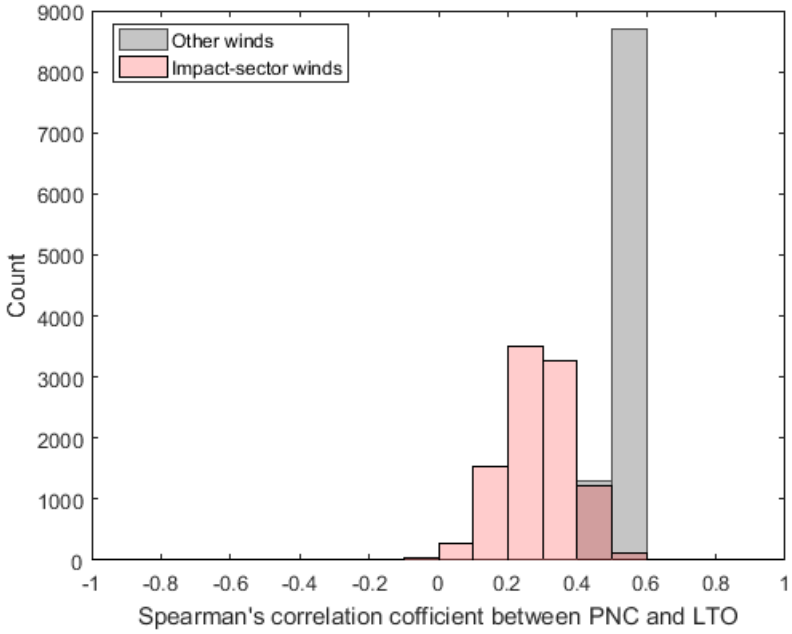

Figure S32: Distribution of bootstrap estimates for Spearman's correlation coefficient between PNC and WS at site C3.

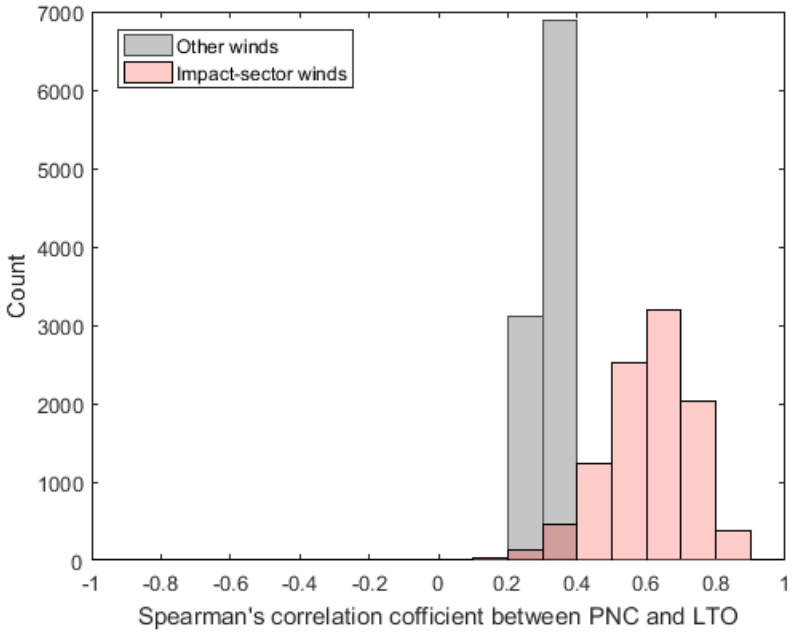

Figure S33: Distribution of bootstrap estimates for Spearman's correlation coefficient between PNC and WS at site B1.

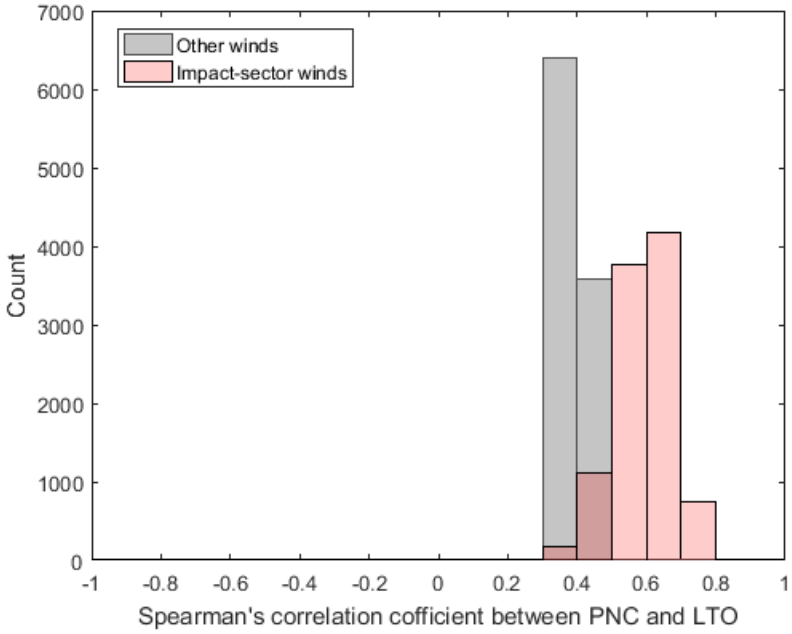

Figure S34: Distribution of bootstrap estimates for Spearman's correlation coefficient between PNC and WS at site B2.

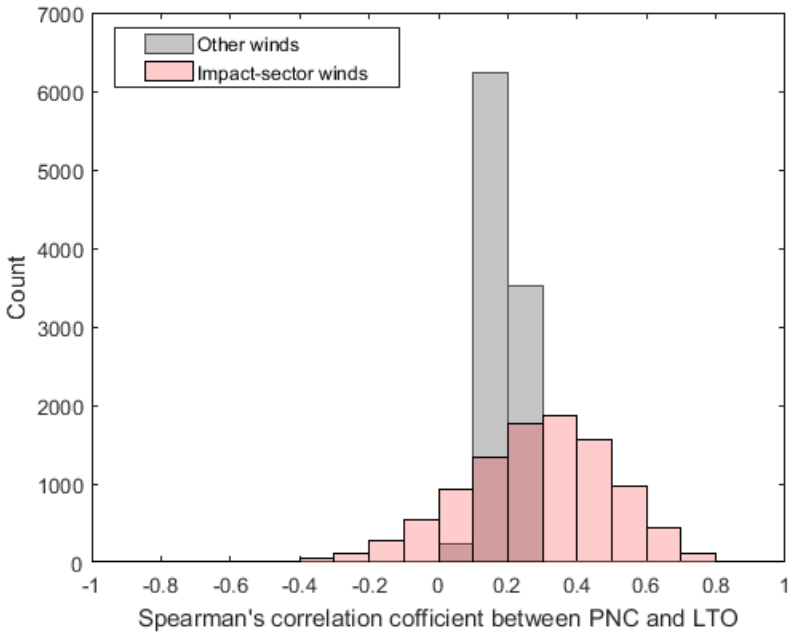

Figure S35: Distribution of bootstrap estimates for Spearman's correlation coefficient between PNC and WS at site B3.

Particle Number Concentrations Trend with respect to Wind Direction

The following figures S36-S42 and S43-S51 show medians per 10-degree-wide sector for hourly median particle number concentration data classified into impact-sector vs other winds. Impact-sector boundaries did not always coincide with the boundary of the 10-degree-wide sectors that were centered on even 10° and spanned ±5°. For such situations, both impact-sector and other wind medians have been plotted for the same 10-degree-wide-sector.

Chelsea Study Area

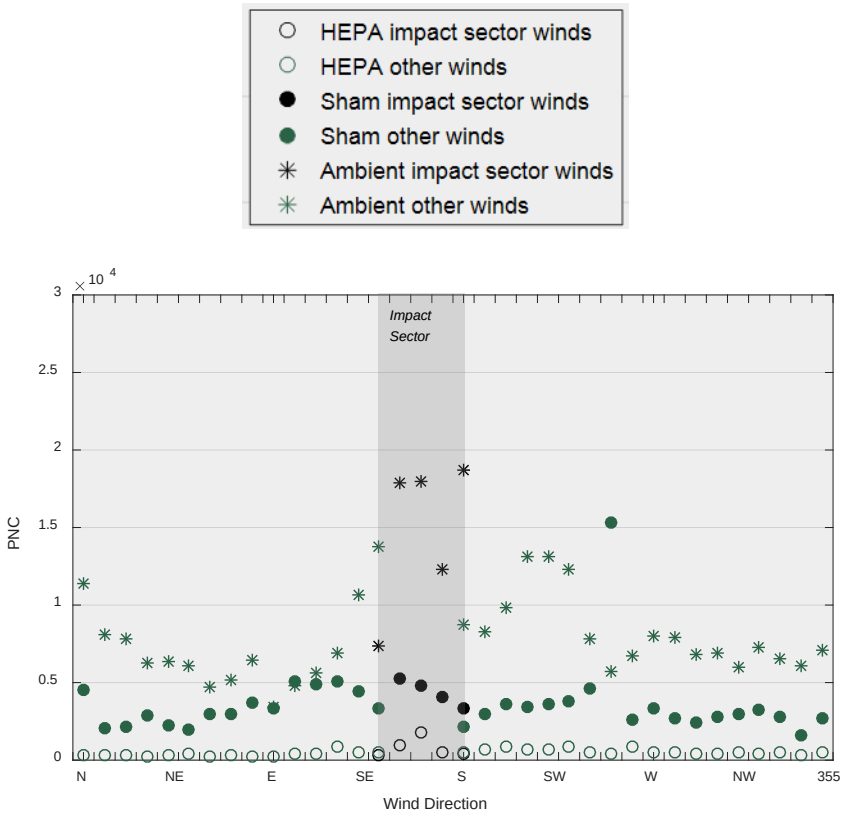

Figure S36: Particle number concentrations (PNC) at site U1 in Chelsea study area.

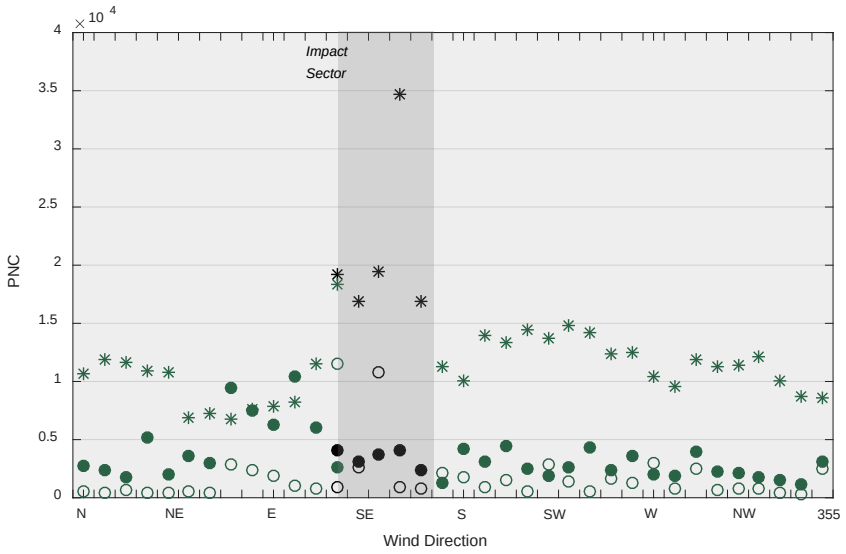

Figure S37: Particle number concentrations (PNC) at site U2 in Chelsea study area.

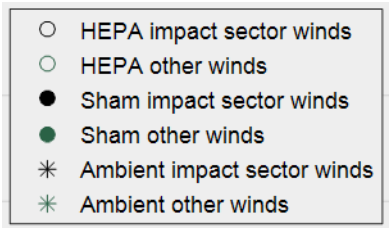

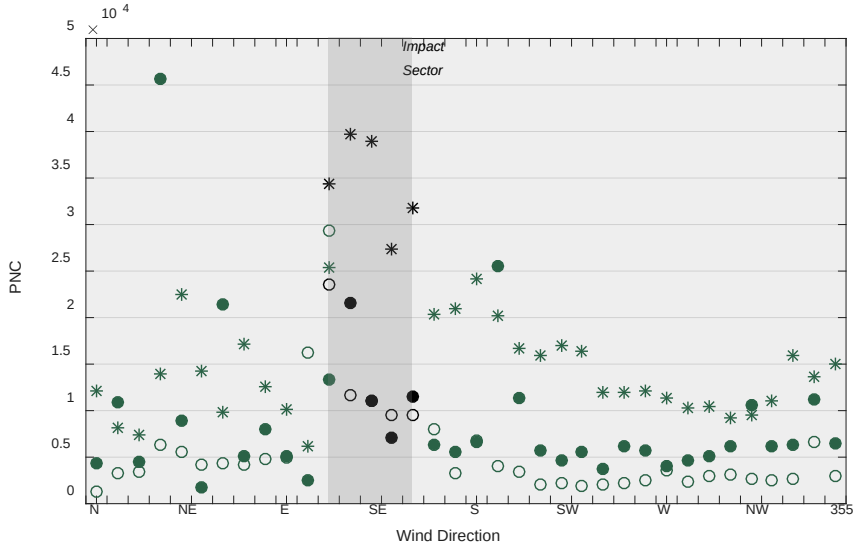

Figure S38: Particle number concentrations (PNC) at site D1 in Chelsea study area.

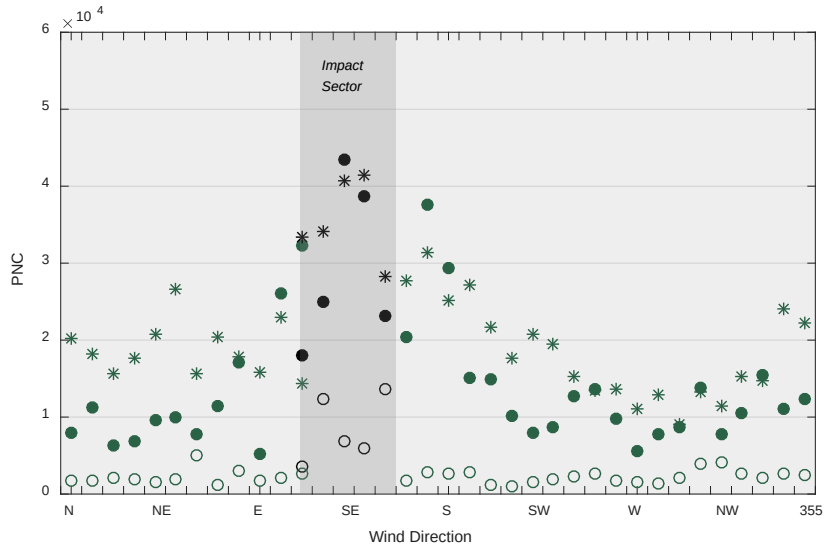

Figure S39: Particle number concentrations (PNC) at site D2 in Chelsea study area.

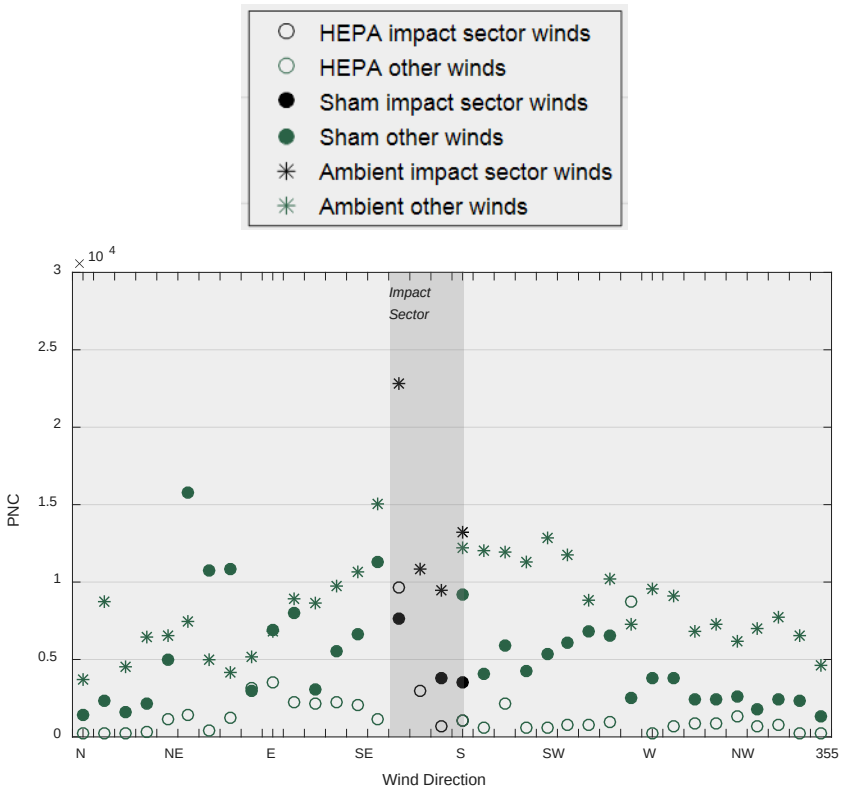

Figure S40: Particle number concentrations (PNC) at site C1 in Chelsea study area.

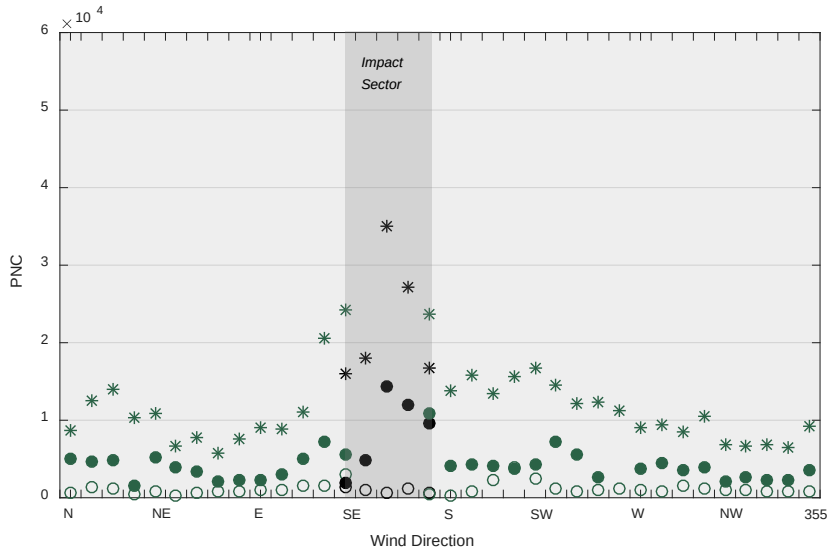

Figure S41: Particle number concentrations (PNC) at site C2 in Chelsea study area.

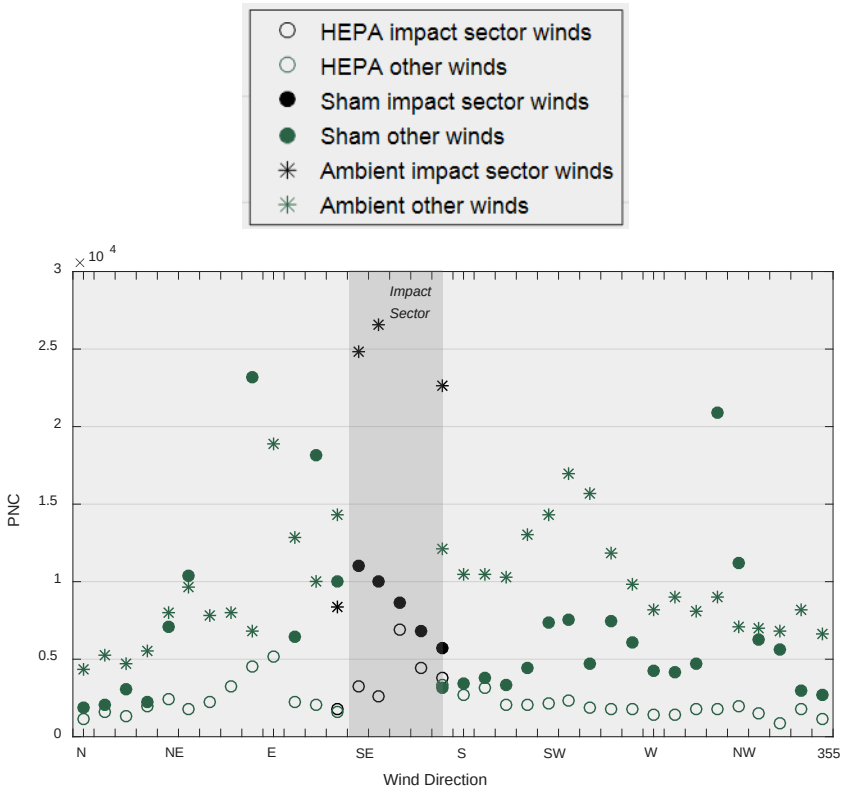

Figure S42: Particle number concentrations (PNC) at site C3 in Chelsea study area.

Boston Study Area

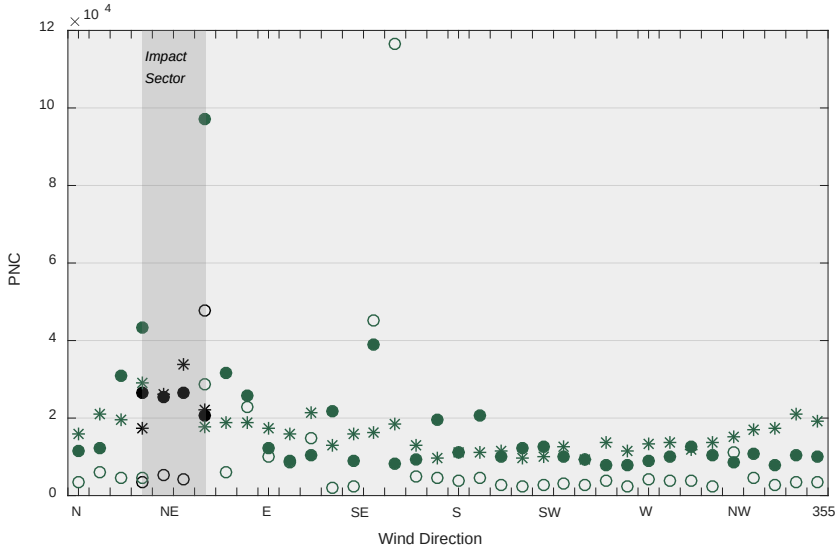

Figure S43: Particle number concentrations (PNC) at site D1 in Boston study area.

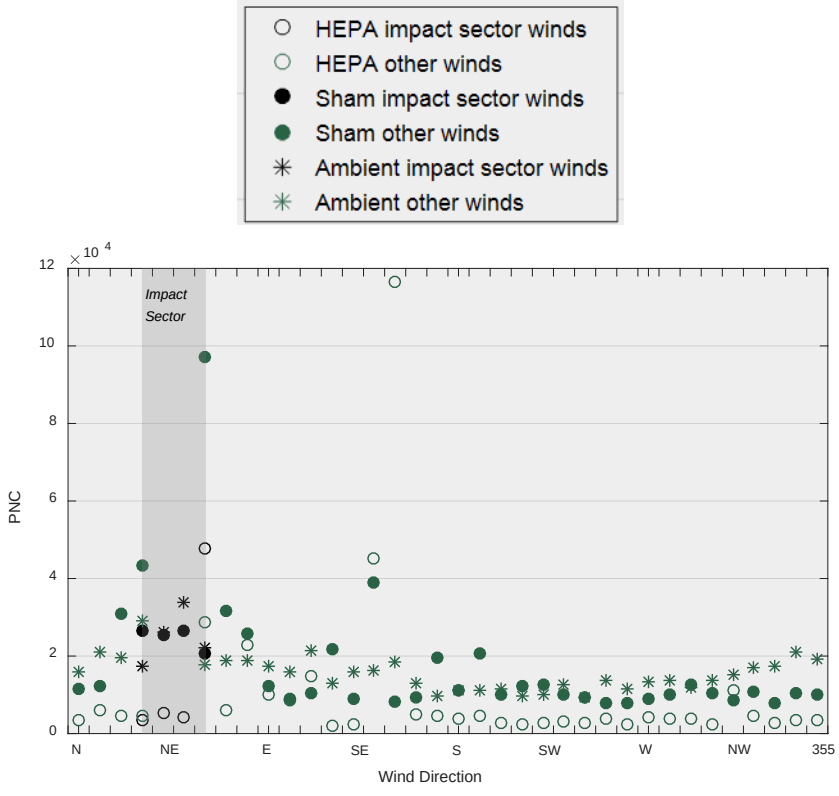

Figure S44: Particle number concentrations (PNC) at site U1 in Boston study area.

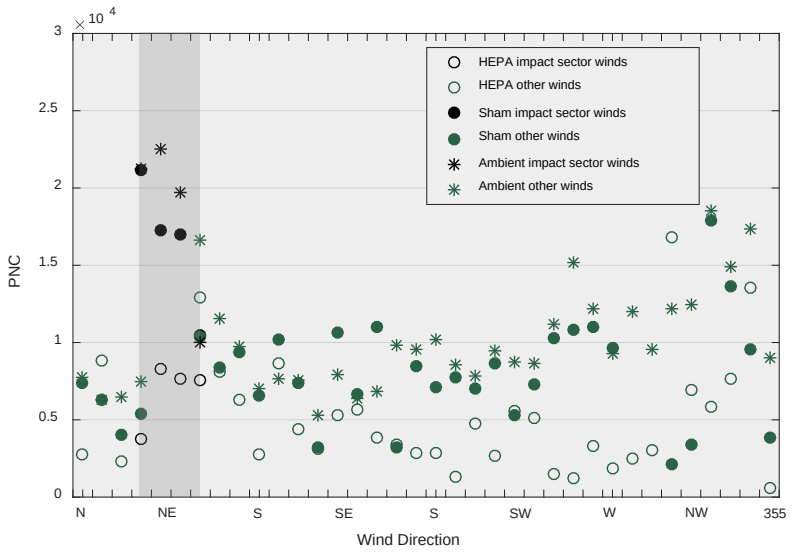

Figure S45: Particle number concentrations (PNC) at site U2 in Boston study area.

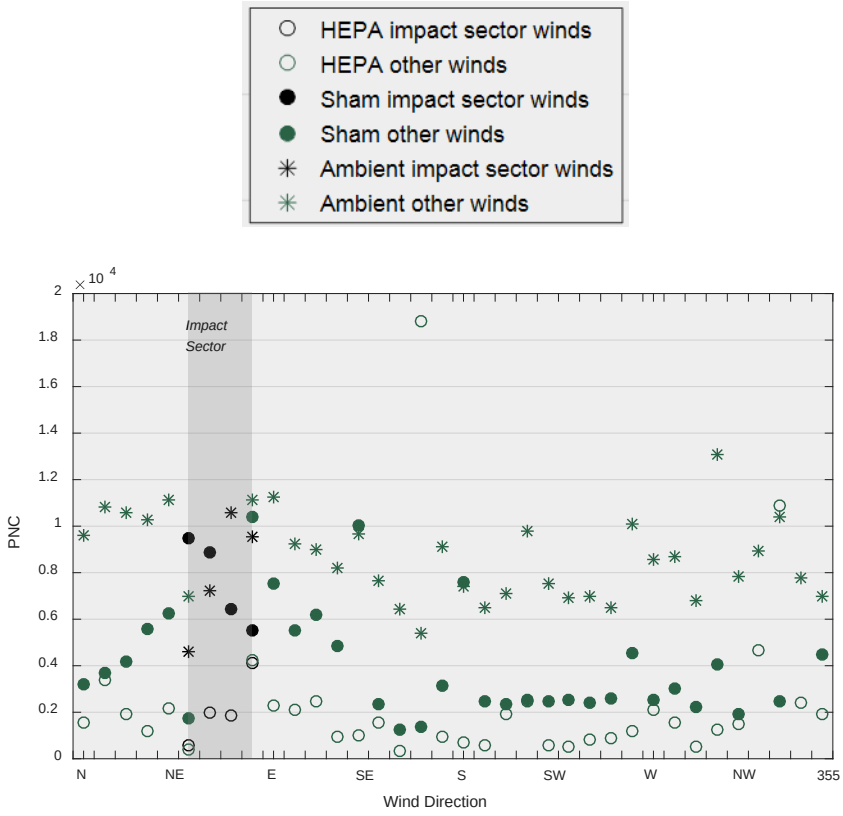

Figure S46: Particle number concentrations (PNC) at site C1 in Boston study area.

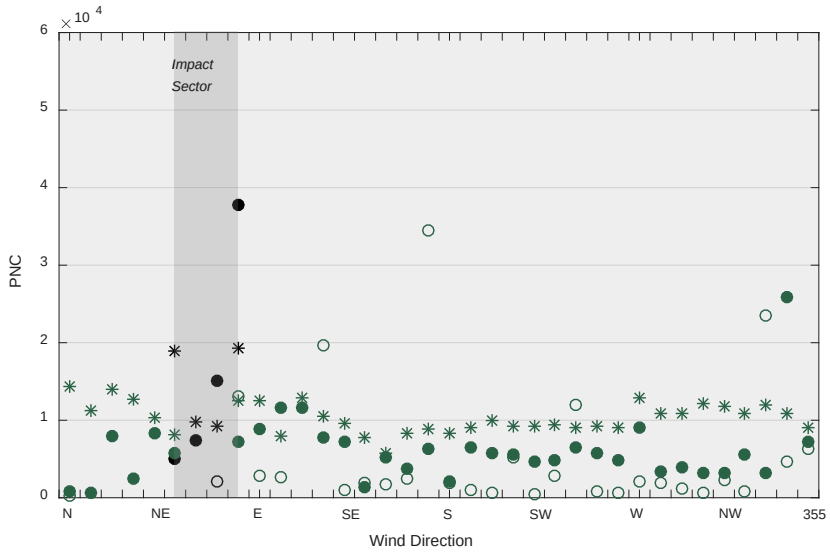

Figure S47: Particle number concentrations (PNC) at site C2 in Boston study area.

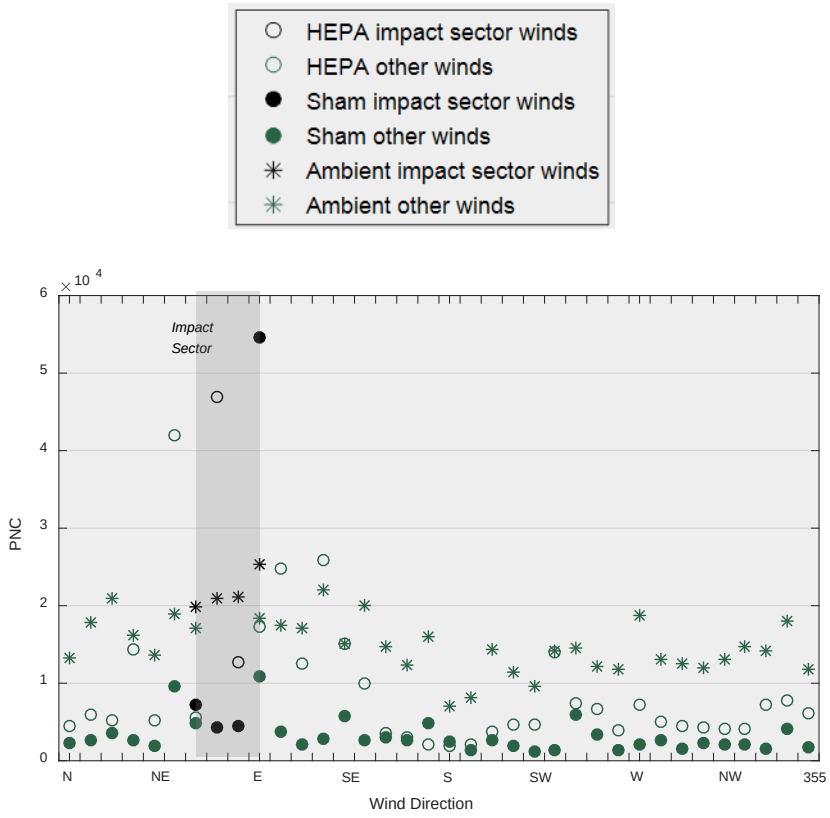

Figure S48: Particle number concentrations (PNC) at site C3 in Boston study area.

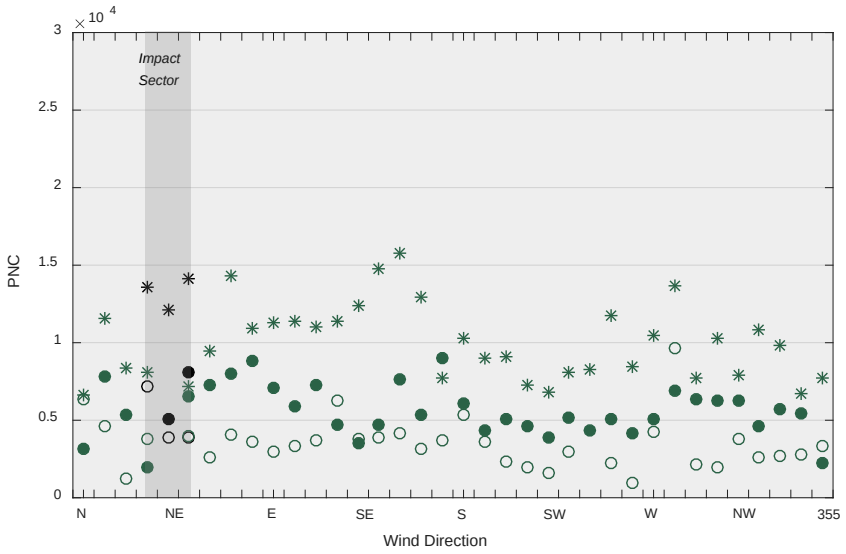

Figure S49: Particle number concentrations (PNC) at site B1 in Boston study area.

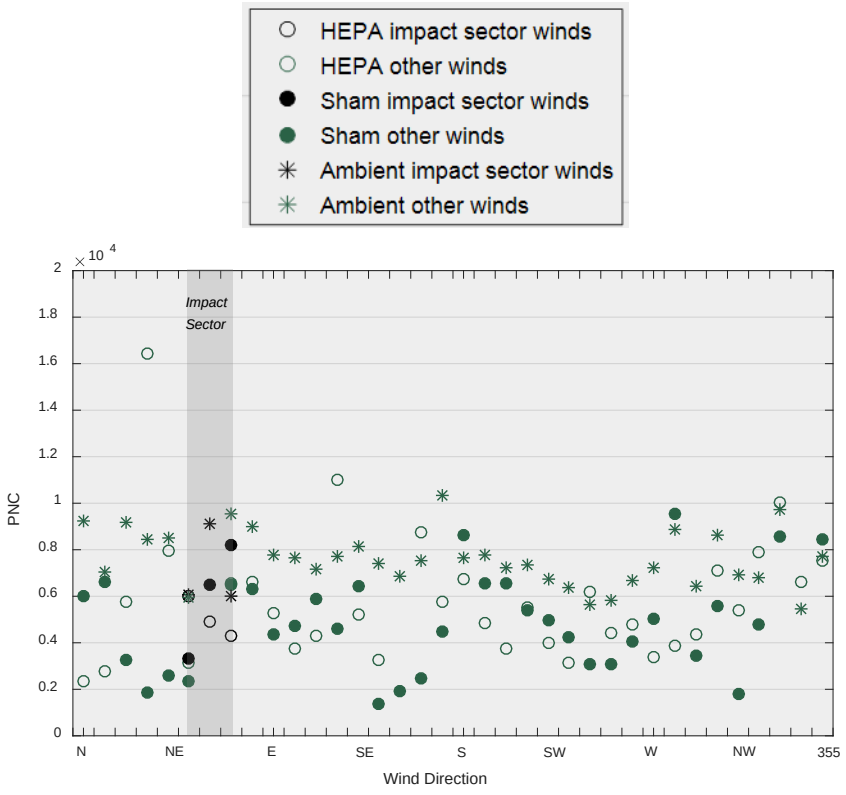

Figure S50: Particle number concentrations (PNC) at site B2 in Boston study area.

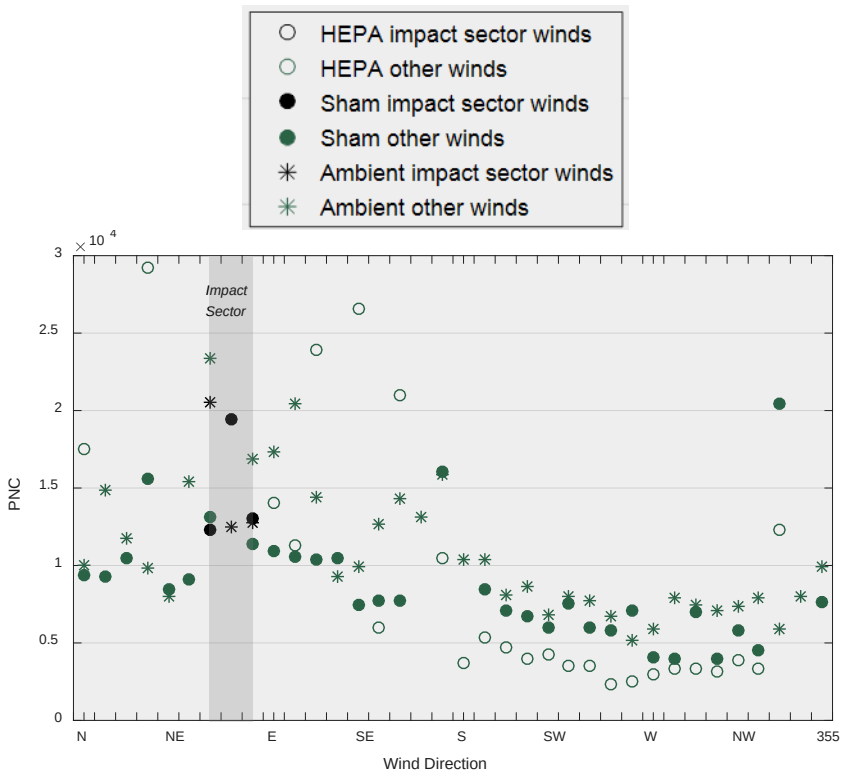

Figure S51: Particle number concentrations (PNC) at site B3 in Boston study area.

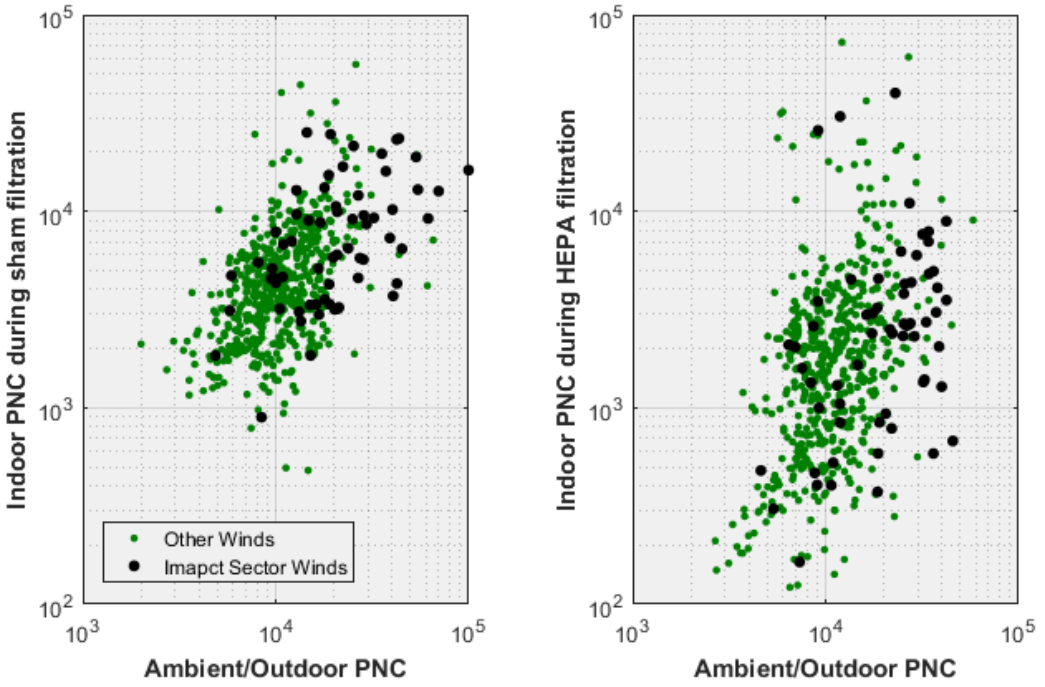

Figure S52: Indoor versus outdoor or ambient concentrations during sham and HEPA filtration. Each point represents the median of hourly minimums classfied into 10-degree-wide-sectors.

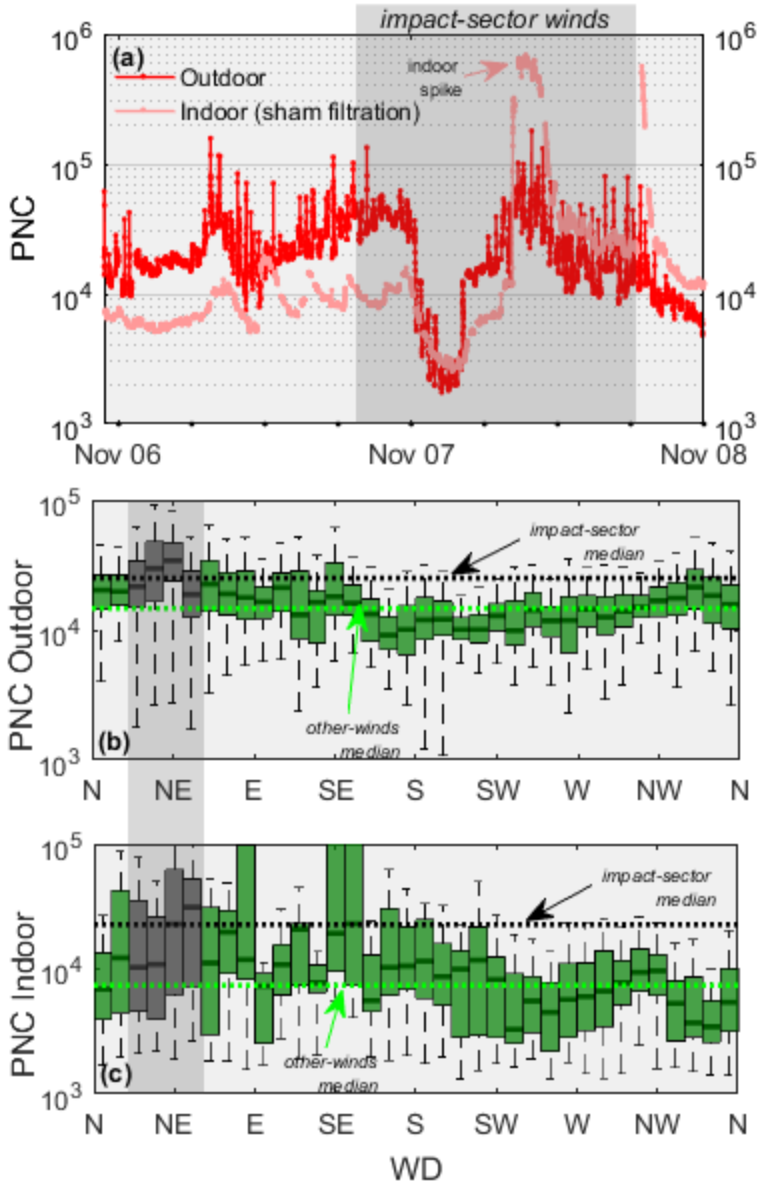

*Figure S53: PNC time series for Nov 6-8, 2012 for site U1 in Boston is shown in (a) and impact-sector winds are highlighted in gray. Tukey's boxplots in (c)-(d) show outdoor and indoor PNC data. The horizontal line inside each box is the median, the boxes extend from the 25th to the 75th percentile and the whiskers extend to 1.5*interquartile range.*